G. H. Schwuttke
T. F. Ciszek
K. H. Yang
A. Kran

Low Cost Silicon for Solar Energy Conversion Applications

Abstract: Economically viable means of producing silicon solar cells for the conversion of solar energy into electric power are discussed. Emphasis is given to the discussion of crystal growth techniques capable of growing single-crystal silicon ribbons directly and inexpensively from molten silicon. The capillary action shaping technique (CAST) recently developed by IBM has a good potential for producing low cost silicon sheets suitable for solar cells. This technique has produced ribbon 100 mm wide and 0.3 mm thick. Problems that CAST must overcome in order to supply material for low cost solar cells are discussed. Economic and technological computer-modeled comparisons indicate that continuously grown CAST ribbons of these dimensions can meet a cost objective below $\$50/m^2$ of sheet material. The results require that it be possible to fabricate a twelve-percent-efficient solar cell from CAST ribbon 100 mm wide and 0.3 mm thick at a polycrystalline silicon cost of \$10/kg.

Introduction

The widespread application of silicon solar cells to photovoltaic energy conversion is presently held back primarily by cost. Today's cost of packaged solar cells capable of generating one peak watt of electricity is between \$15 and \$20. Department of Energy (DOE) officials assert that this cost must come down to \$0.50/W for cells to compete with conventional energy sources. The goal is to achieve this cost figure in 1986.

In addition to this capital cost of \$15 000 per peak kW of generating capacity for a solar cell system in a central generating station, provisions must be made for energy storage. Storage capacity for three to six hours of the station's output would increase the total system cost to \$30 000 to \$50 000 per peak kW. For such a system to compete with fossil-fueled or nuclear power plants, it is estimated that the cost must be reduced to \$1000 per peak kW (all cost goals are given in 1975 dollars).

In producing electricity from solar cells, most of the expense is related to obtaining material of sufficient purity for the manufacture of the cells. Solar cells are predominantly fabricated from silicon, the second most abundant element on earth. In its purest form it is found in quartz and quartzite. Obtaining silicon from quartzite in the needed purity is a very expensive process, but efforts are being made to shrink this expense. Research sponsored by DOE is aimed at producing solar-grade polycrystalline silicon in excess of 3000 metric tons per year (1 metric ton = 10^3 kg) at less than \$10/kg by 1986. The selection process involved in this research examines and re-examines past processes for preparing silicon as well as those currently in commercial use. In addition, over 200 chemical reactions have been considered by which

Figure 1 Die for CAST ribbon growth. (a) Top view; (b) side view with cutaway.

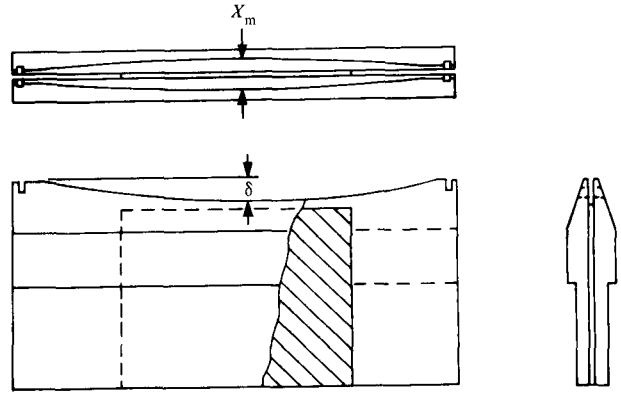

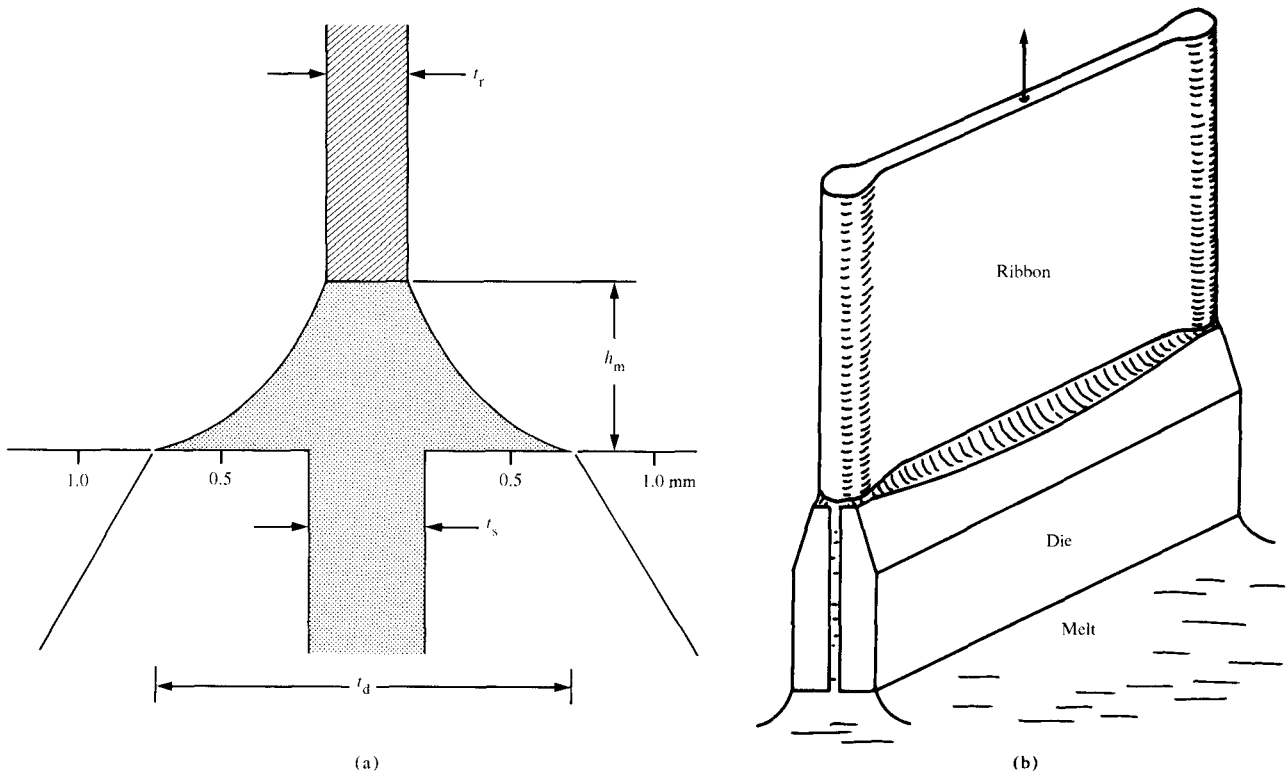

Figure 2 (a) Cross-sectional view of meniscus configuration; (b) illustration of the high melt meniscus growth in CAST ribbons.

the preparation of silicon might be possible through the reduction of readily available compounds. Today, upgrading the arc-furnace process for making metallurgical-grade silicon is deemed the most probable means of meeting DOE goals for solar-grade silicon.

The second major solar cell expense is in the fabrication of the wafers from Czochralski-grown silicon crystals or boules, which is a wasteful and expensive process. One-half to two-thirds of the boule is lost in saw kerfs and polishing operations. In addition, large parts of the solar cell manufacturing process involve batch operation.

A process for continuous growth of ribbon crystals is envisioned to permit continuous, automated device fabrication, overcoming wasteful manufacturing processes and thus substantially reducing costs. Many attempts have been made to provide such a solution, including the dendritic web process [1, 2], the Stepanov technique [3] as applied by Boatman and Goundry [4], and the edge-defined film-fed technique [5–8] first applied to silicon by Ciszek [9] and subsequently improved by Ciszek and Schwuttke [10, 11].

Ribbon growth programs in the United States aim at continuous growth of silicon ribbons at high growth rates (75 mm/min). The ribbons should be 100 mm wide and 0.3 mm thick, with a solar cell conversion efficiency of better than ten percent. In anticipation of this goal, we are involved in a research program pursuing the growth of silicon ribbons by a capillary action shaping technique (CAST), as described in [10, 11]. Recently, this work has achieved ribbon widths of 50 mm for a length of over 1 m and 93 mm for a length of 0.17 m. Ribbons of such widths were grown with an average thickness of 0.3 mm at a growth speed of over 30 mm/min. Although considerable progress has been made with this technique, problems remain that must be solved in order to meet the DOE goal; some of these are addressed in this paper. In addition, details on minority carrier lifetime and solar cell performance of these silicon ribbons are presented, and an economic outlook for their potential for meeting the DOE goal of \$0.50/W is given.

CAST crystal growth method

The crystal-growth method under investigation is a capillary action shaping technique. Meniscus shaping for the desired ribbon geometry occurs at the vertex of a wettable die. As ribbon growth depletes the melt meniscus, capillary action supplies replacement material. The configuration of the technique used in our initial studies was similar to the edge-defined, film-fed growth (EFG) process described by LaBelle [5]. This crystal-growth method has been applied to silicon ribbons for several years [9]. As our work on silicon ribbon growth progressed, we

found that substantial improvements in ribbon surface quality could be achieved with a melt meniscus higher than that attainable with the EFG technique. Thus, in our present work we have abandoned the EFG technique in favor of the improved capillary action shaping technique CAST [10, 11], which makes use of the capillary die design shown in Fig. 1.

This technique represents a departure from the die types used for edge-defined film-fed growth, in that the bounding edges of the die top are not parallel or concentric with the growing ribbon. The new die allows a higher central melt meniscus [Figs. 2(a, b)], concomitant improvements in surface smoothness, and freedom from SiC surface particles that can degrade perfection.

In addition, the CAST growth system provides a novel approach to growing wide silicon ribbons through thermal profile control that is continuously variable, inert, and capable of heat extraction [11]. In this device, multiple inert-gas jets, each with an individually controlled flow adjustment, are directed to various parts of the hot zone.

The CAST die shown schematically in Fig. 1 is typical for our die design. It is about 1.9 mm thick in the mid-region (X_m), with a 1.5-mm deviation from flatness (δ) that produces a central ribbon thickness of about 0.3 mm for an overall die thickness t_d of 50 mm or larger. The meniscus height h_m under these conditions is about 0.7 mm. The relative dimensions of ribbon, die, and meniscus are given in Fig. 2(a); these dimensions are given here in mm. Note: the ribbon thickness t_r is different from the die thickness t_d and the capillary slot thickness t_s. The high central-melt meniscus provided by this die design results in smoother ribbon surfaces and greater freedom from β-SiC surface particles that can degrade perfection [10].

Because of transverse variations in die thickness, die height, and meniscus volume, dynamic control over the temperature distribution in the growth region is desirable. The inert-gas thermal balancing system provides the thermal control necessary for growing stable ribbons as wide as 100 mm and has made possible full-width seeding of such ribbons.

Figure 3 shows a silicon ribbon 50 mm wide being grown by the CAST technique, with inert-gas jet control for thermal adjustments at each ribbon edge. The high central-melt meniscus (black, thin crescent) promotes smooth, reflective ribbon surfaces.

Since the gas jets are directed toward the growth region, it has been possible to use an open pulling port system and still retain clean ribbon surfaces of a type heretofore obtained only in a closed, gas-tight growth system.

The system has been used to grow more than sixty silicon ribbons 38 and 50 mm wide and up to 1.2 m long, and it has provided the necessary thermal balancing for good width control. It has been particularly beneficial in maintaining a high melt meniscus for the growth of ribbons

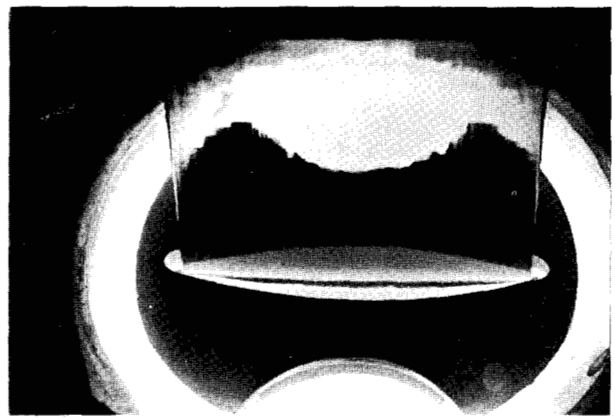

Figure 3 CAST-grown 50-mm-wide silicon ribbon, where inert-gas jets are used for thermal adjustments at each edge of the ribbon. The high central-melt meniscus (black, thin crescent) promotes smooth, reflective ribbon surfaces.

with low silicon carbide surface particle densities ($9 \times 10^{-3}/cm^2$). In addition, crystals grown with a high melt meniscus display relatively large grains, several mm in size. These also displayed excellent minority carrier lifetime distributions.

Recently a system for 100-mm ribbons has been successfully implemented.

- *Die problems*

During silicon ribbon growth, particularly without thermal jet control, small SiC crystallites may form in the orifice of the die. Such crystallites are also found floating in the meniscus at the top of the die. Such a particle frequently becomes attached to the silicon ribbon, destroying its perfection [10].

Similar deposits are observed on the outside of a carbon die in contact with the molten silicon. An accumulation of crystallites is shown in the orifice of a carbon die in Fig. 4(a) and on the outside of a die in Fig. 4(b). Scanning electron micrographs of such small crystals scraped from the orifice and from the side of the die are shown in Fig. 5. These crystals appear equiaxial and expose mainly (111) and (100) surfaces. The morphology of the SiC crystals is in agreement with growth by precipitation from a liquid phase. Some of these crystals are found in clusters bonded to each other within a very limited area where the crystal orientations are identical. It is obvious that small SiC crystals of high crystallographic quality can be grown by this technique as a byproduct (in this case, unwanted) of Si ribbon pulling.

CAST ribbon quality

Ribbon crystals grown by the capillary action shaping technique display a unique defect structure. Under steady state growth conditions, the defect structure is dominated

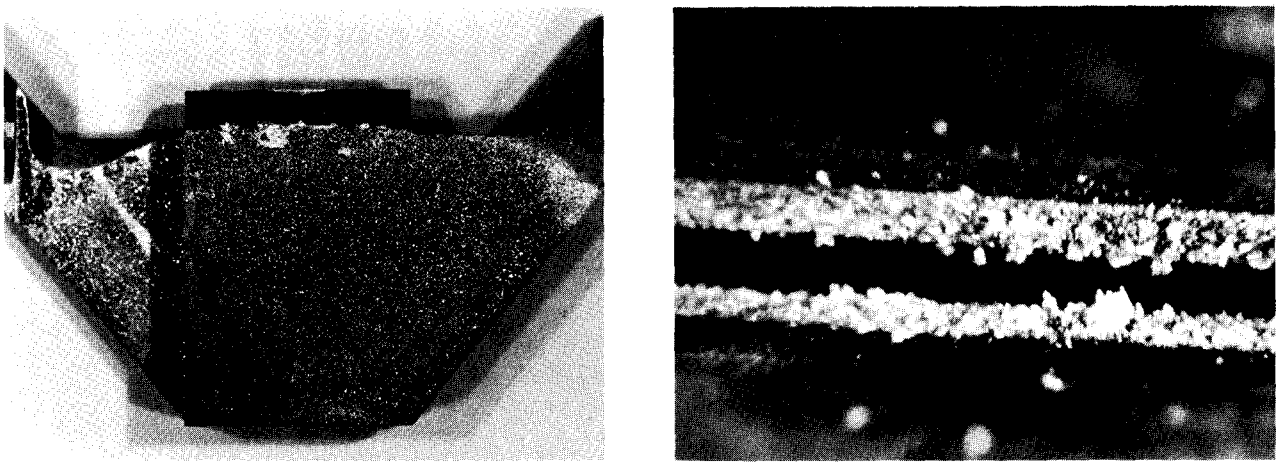

(a) (b)

Figure 4 Accumulation of SiC (a) on outside and (b) in orifice of carbon die.

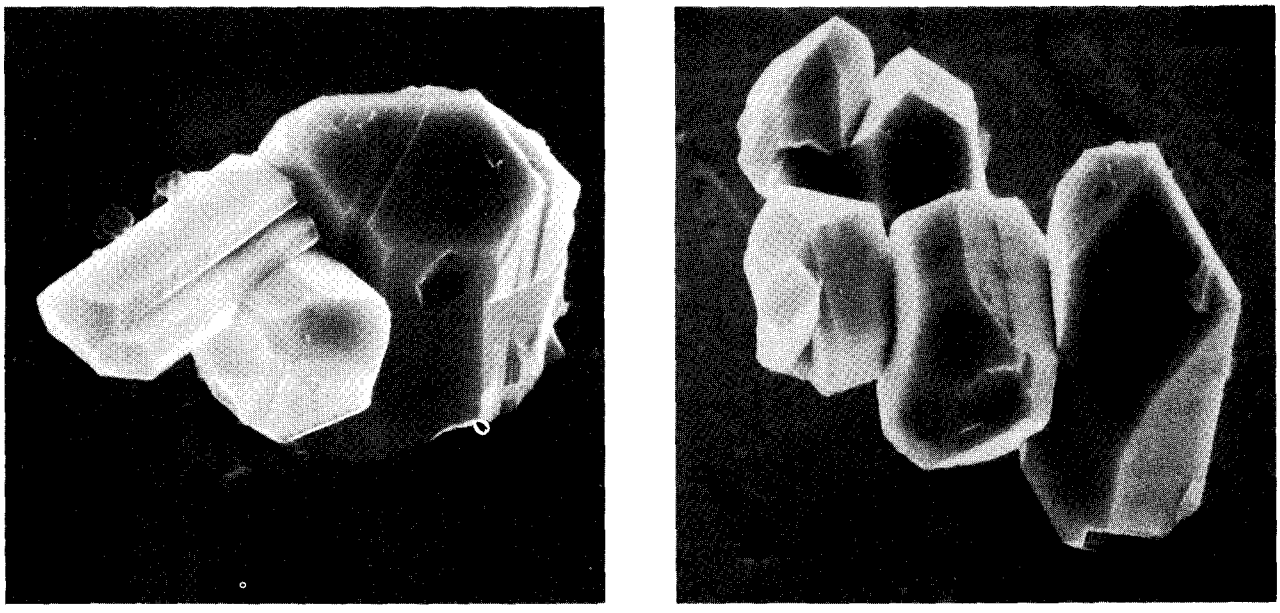

Figure 5 Scanning electron micrographs of SiC crystals scraped from orifice of carbon die.

by linear boundaries parallel to the ribbon edges [12]. The best ribbons obtained have a surface orientation close to (011) and boundaries in the ⟨211⟩ growth direction [12]. Seed orientation has no influence on the steady state growth perfection of the ribbon. The electrical effects associated with the equilibrium defect structure are of interest because they influence solar cell efficiency [12]. The electrical activity of ribbon defects can be investigated qualitatively through use of the electron-beam-induced current (EBIC) signal in the scanning electron microscope while the influence of defects on minority carriers can be measured quantitatively through metal oxide semiconductor capacitance vs time (MOS *C-t*) measurements.

• *EBIC measurements*

The EBIC technique is useful for nondestructive imaging of electrically active defects in silicon. Electron-beam-in-

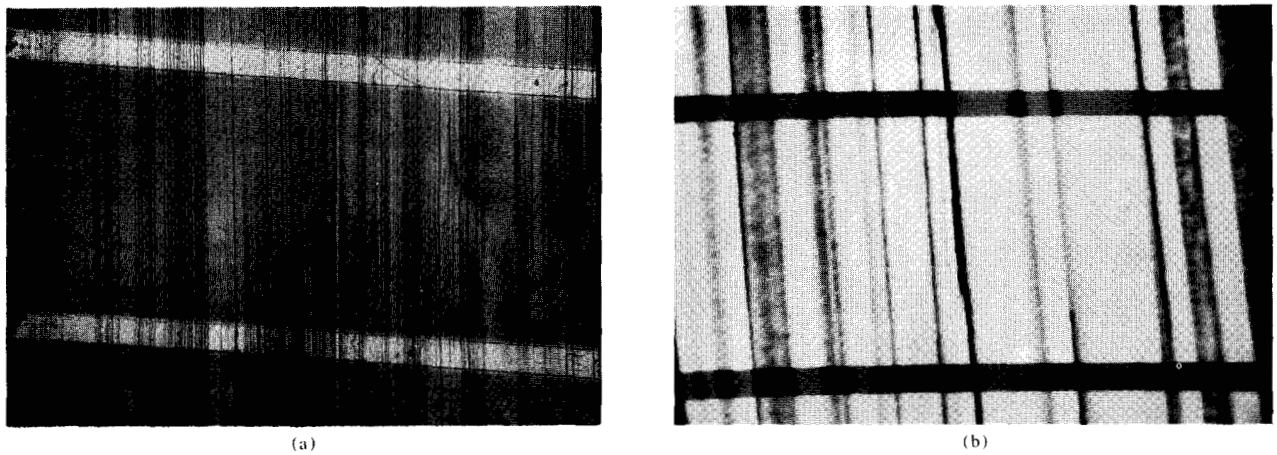

(a) (b)

Figure 6 (a) Optical and (b) SEM EBIC micrographs of a silicon ribbon solar cell; magnification is 20× for both, e-beam power is 30 keV.

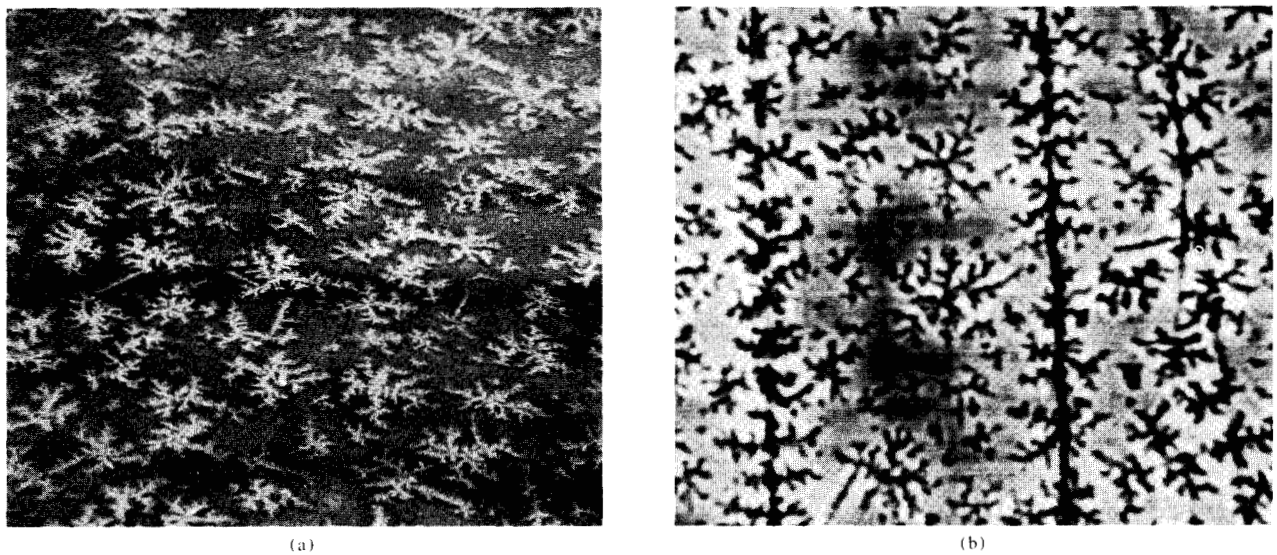

(a) (b)

Figure 7 Scanning electron micrographs of a silicon ribbon surface; (a) surface picture showing SiC dendrites (20 keV), and (b) EBIC picture of same surface. Magnification is approximately 1000× for both pictures.

duced current investigations of as-grown ribbons are made with Schottky contacts [13]. Solar cells are investigated in the EBIC mode through use of diffused p-n junctions [14].

The electrically active defect density in a ribbon crystal can be considerably lower than its total defect density. The total defect density is found by Sirtl etching and by optical microscopy of the ribbon surface.

Figure 6(a) shows an optical micrograph of a ribbon solar cell section. The two fingers of the Al-Ag metal grid are visible and can be used for area identification. The parallel lines perpendicular to the fingers are the linear boundaries typical for ribbons grown under steady state conditions. Note the high density of lines. Figure 6(b), the corresponding EBIC picture, shows the Al-Ag fingers as dark horizontal lines. The dark vertical lines and bands in the EBIC picture indicate a local reduction in the beam-induced current when the beam scans over these areas. This is caused by crystal defects that act as preferred recombination centers. The dark bands correlate well with crystal sections that show etch pits (dislocations) after Sirtl etching, while the sharp boundary lines correspond to electrically active twin or grain boundaries. The areas that appear white in the EBIC picture are free from electrically active defects and have better lifetimes than the areas that appear dark.

In addition to dislocations and planar boundaries, SiC dendrites also cause minority carrier lifetime degradation

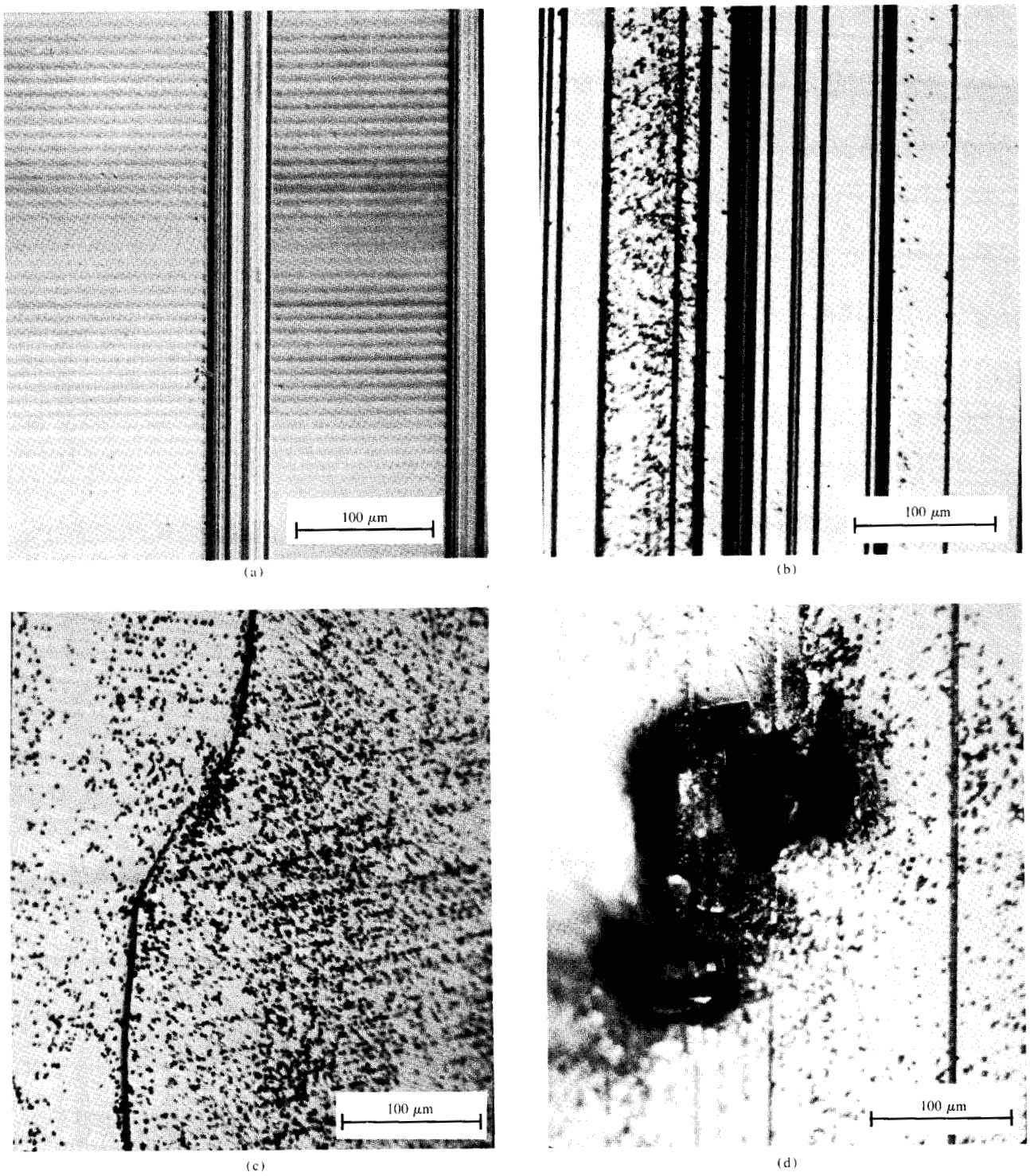

Figure 8 Magnified (250×) sections of silicon ribbon having varying degrees of crystal quality and ranges of minority carrier lifetimes; (a) high quality, 1–10 μs lifetimes; (b) twinning and dislocations present, 0.01–1 μs; (c) small-angle grain boundary present (note dislocation pits), <0.01 μs, and (d) SiC inclusion present, lifetime not measurable because of leaky oxide.

in ribbons [see Figs. 7(a) and (b)]. The scanning electron microscopic (SEM) surface image of dendrites covering the ribbon surface is shown in Fig. 7(a), while the corresponding EBIC image, with p-n junction contrast, is given in Fig. 7(b). Such dendrites act as highly effective recombination centers. The efficiency of solar cells is reduced to the one-to-three-percent range if such dendrites are present in large numbers.

• *Minority carrier lifetime measurements*

The EBIC measurements are in good qualitative agreement with MOS *C-t* lifetime [15] data obtained from such crystals. Minority carrier lifetime values of typical defect areas are obtained by placing MOS capacitors in these areas. The lifetime degrading property of a particular defect pattern can be measured directly in this way. A comparison of the EBIC picture and the lifetime data is also possible because the same MOS capacitor can be used for EBIC display and lifetime measurements. Examples of lifetime variations and their dependency on ribbon perfection are shown in Figs. 8(a–d). Figure 8(a) illustrates a ribbon section of high quality crystal structure. The crystal section between the twin boundaries is nearly perfect. One section of lesser quality, containing twins, is shown in Fig. 8(b). Note the etch pits indicating dislocations in the left and right crystal section. The middle section between the twin boundaries is free of etch pits. Other defect configurations found in steady-state-grown ribbon sections are shown in Figs. 8(c) and (d). A small-angle grain boundary is shown in Fig. 8(c). Note the dislocation pits to the right and left of the boundary. A SiC surface inclusion is shown in Fig. 8(d). The measured lifetimes noted for each defect pattern represent typical data.

The lifetime of minority carriers in ribbons varies with the position of the MOS dots relative to the edges of the ribbon. Longer lifetimes are found for dots located in the center of the ribbon, rows K–Q, as illustrated in Fig. 9. This figure also summarizes lifetime measurements made for three different crystals. The ordinate gives the minority carrier generation lifetime in microseconds; the abscissa gives the position (row identification) of the MOS dot relative to a ribbon edge. The dots A and W are close to the left and right edges of the ribbon, respectively. The solid line in the figure indicates the average lifetime values (obtained by plotting averaged single-lifetime values per column against the distance from the edges) for the different ribbon sections. The ratio of the average lifetime for dots located in the middle of the ribbon to those for dots located close to the edges can be as large as 200. Perfection studies made on these ribbon sections indicate that the lifetime degradation correlates with the crystal structure quality, which improves toward the center of the ribbon.

Lifetime values larger than 500 μs have been measured in defect-free sections of CAST ribbons, which indicates that ribbons grown from carbon dies have potential for high-efficiency solar cells.

β-SiC dendrites have been found to deposit epitaxially on ribbon surfaces during ribbon growth. The density of such dendrites is highest near the seed-ribbon interface, decreasing rapidly with increasing distance from the interface. These dendrites have been found, by means of EBIC measurements, to cause serious lifetime and solar

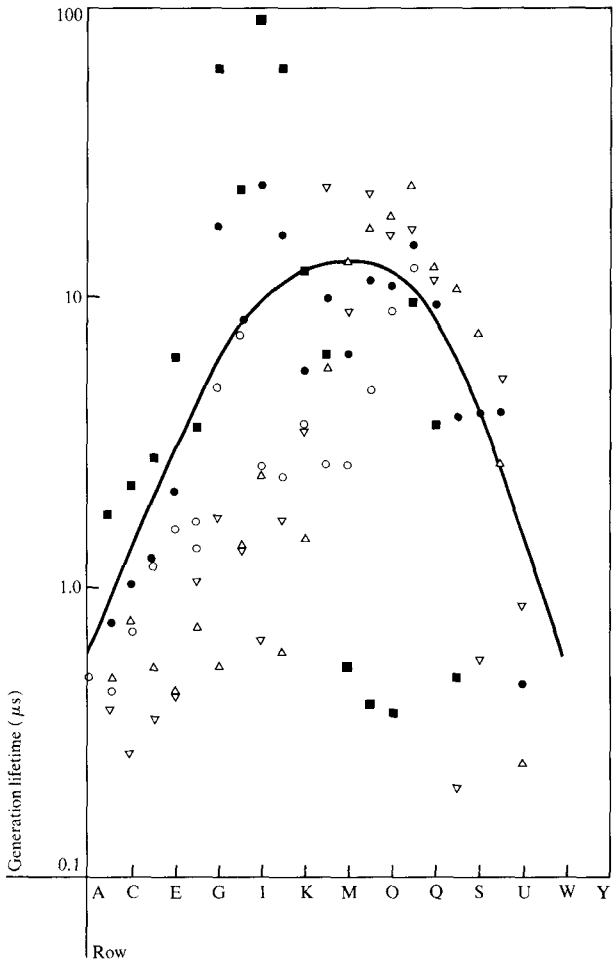

Figure 9 Lifetime variation across ribbon surfaces. Ribbon sections were tested at various distances (cm) from the seed crystal: 20, ○; 36, △; 48, ■; 60, ▽; averages of these lifetimes for each row are indicated by ●.

cell problems such as leaky MOS devices and low efficiencies. This problem is eliminated by removing a thin layer (10 μm) of the as-grown surface through etching in an acidic mixture (3 HNO_3 : 1 HAc : 1 HF). Etching the ribbons before processing also relieves the problem of breakage, which is more pronounced for the as-grown ribbons.

Results of lifetime measurements made on as-grown ribbons and on ribbons slightly etched before processing are summarized in Table 1. It can be seen that, due to the presence of β-SiC dendrites, the occurrence of leaky MOS dots can be very high on ribbon sections cut as far as 400 mm from the interface. Etching before processing eliminates this problem.

Classification of CAST ribbon quality

The conversion efficiency of silicon solar cells depends on a variety of factors and their complex interactions. Most

Table 1 Influence of β-SiC dendrites on lifetime of silicon ribbons.

Ribbon type	*Distance from seed* (cm)	*MOS dot size* (mm)	*Range of lifetime* (μs)	*Average lifetime* (μs)	*Relative area containing Sic* (%)
			Ribbon A		
As-grown	6–12	0.5	0.011–10.5	2.26	68
As-grown	18–24	0.5	0.001–1.64	0.20	52
As-grown	30–36	0.5	0.005–6.48	1.07	31
		1.5	0.081–1.13	0.34	58
As-grown	42–48	0.5	0.020–52.7	2.50	12
		1.5	0.028–2.42	0.44	21
			Ribbon B		
As-grown	Unknown	0.5	0.0003–0.096	0.034	77
Etched	Unknown	0.5	0.039–44.3	6.54	0
Etched	Unknown	1.5	0.011–29.0	5.93	0

Table 2 Classification of ribbon quality.

Class	*Lifetime range* (μs)	*Solar cell efficiency*[a] (%)	*Dominant defects*
I	1–10	5–8	Coherent twins, stacking faults, dislocations below $10^4/cm^2$.
II	0.01–1	3–5	Noncoherent twins, multiple stacking faults, low angle grain boundaries, dislocations above $10^4/cm^2$.
III	<0.01	1–3	Grain boundaries, dislocations above $10^6/cm^2$.
IV	Not measurable	—	Silicon carbide dendrites on surface.
Standard Czochralski wafer	10–500	8–12	None

[a]Measured at AM1 (a term for the average solar spectral radiance at the earth's surface on a bright sunny cloudless day), no antireflective coating.

important is the presence or absence of nonradiative recombination centers. The presence of transition metals in the silicon also has a great influence on solar cell efficiencies. Finally, there is evidence that crystallographic defects in silicon can influence solar cell efficiency. Therefore, we have classified ribbon quality according to the influence of dislocations and other ribbon defects on generation lifetimes and solar cell efficiencies.

Dislocations in ribbons are either randomly distributed throughout the grains or aligned in the slip directions. Transmission electron microscopic investigations of ribbons with (011) surface orientation show these dislocations to have Burgers vectors $a/2$ (110) parallel or inclined to the (011) ribbon surface. For such dislocations one finds that the product of lifetime τ and dislocation density N_D is approximately 0.5 s/cm^2. This is a factor of 30 lower than that reported for grown-in dislocations in float-zone silicon of 1000 ohm-cm resistivity [16]. Assuming that the lifetime-measurement technique (photovoltaic decay) used in [16] and the MOS *C-t* technique [15] give comparable results for the bulk lifetime, this τN_D value would indicate that the electrical activity of 60° dislocations in ribbons is higher than the electrical activity of grown-in dislocations in float-zone crystals. This conclusion appears reasonable.

Transmission electron microscopic investigations of electrically active and inactive boundaries were also made [17]. These investigations indicate that all inactive boundaries are either first-order (coherent) twin boundaries or are composed of multiple stacking faults. The electrically active boundaries are found to contain varying numbers of dislocations; the electrical activity of such boundaries depends on the number of dislocations present.

On the basis of electrical measurements and detailed structural investigations [17], ribbon quality is classified as shown in Table 2. Four different categories of crystal quality are defined, and these are based on a correlation between the lifetime ranges and the observed solar cell efficiencies. The classification is also based on a large volume of experimental data and represents a reasonably accurate guideline to ribbon quality and to the resulting influence on solar cell efficiency.

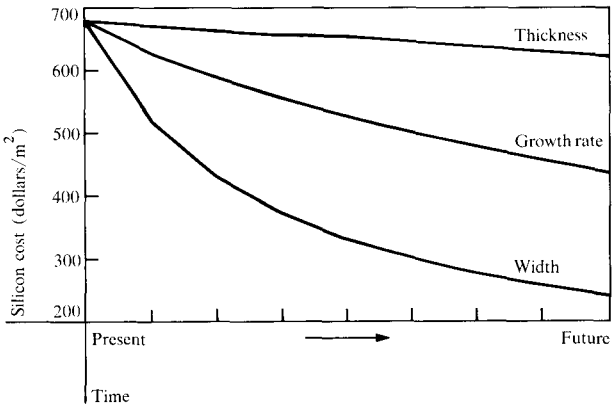

Figure 10 Single-ribbon system sensitivity analysis: silicon sheet cost vs time for processing-technology parameters.

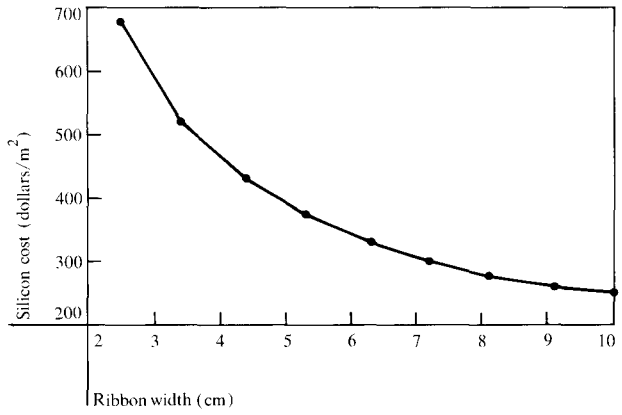

Figure 11 Single-ribbon system: silicon sheet cost vs ribbon width.

The correlation between lifetime and solar cell efficiency shown in Table 2 is interesting. Each lifetime range corresponds to a specific range of solar cell efficiencies. Note that the standard Czochralski wafer (defect-free) has the best lifetime and also the best solar cell efficiency. In this context we believe that "high-efficiency" solar cells may require a well controlled defect state in the silicon material.

Economic and technological outlook

We now present the economic-technological requirements for ribbon technology prerequisite for the DOE 1986 energy-capacity-cost goal. This \$0.50 goal relates to a sheet material cost of approximately \$25/m^2 for silicon 0.3 mm thick, and requires a 12–13 percent solar cell conversion efficiency. This is an ambitious requirement for any material technology. On the basis of our findings, we feel that the silicon CAST ribbon technology holds great promise for achieving this goal.

First we look at certain economic considerations that require improvements in processing technology. Such improvements can be achieved without technological breakthroughs. We then discuss the directions that future CAST ribbon development must take in order to meet the DOE goal.

- *Economic outlook*

Processing technology improvements in increasing ribbon widths and growth rates and in decreasing ribbon thicknesses are the key elements for reducing the cost of sheet silicon [18]. Such tasks must be pursued if sheet material costs are to be minimized. For instance, Fig. 10 shows that for present ribbon technology, increasing ribbon width from 25 to 100 mm has the most pronounced effect on reducing the cost of silicon sheet material from \$678 to \$247/m^2. On the other hand, the effect of reducing ribbon thickness alone is relatively small. Increasing the ribbon growth rate from the present 1.5 m/h (thirty percent of the theoretical maximum) to 2.5 m/h (fifty percent of maximum) would have an intermediate effect (see Fig. 10).

An additional perspective for today's technology is provided in Fig. 11, where the cost of silicon sheet material is plotted vs ribbon width [18]. It should be noted that increasing the ribbon width from 25 to 50 mm reduces the sheet material cost from \$678 to \$390/m^2. This cost projection is based on existing technology: 25-mm ribbon width, 1.5 m/h growth rate, \$65/kg polycrystalline silicon cost, 0.3-mm ribbon thickness, and an eight percent ribbon solar cell efficiency.

To approach the DOE \$0.50/W goal, the following technology must be implemented: 100-mm ribbon width, 3.8 m/h growth rate, (75% of maximum), \$10/kg polycrystalline silicon cost, 0.3-mm ribbon thickness, and twelve percent ribbon solar cell efficiency.

Current technology already has the potential for producing sheet material for approximately \$50/m^2 [19]. This is only twice the cost of the DOE goal and looks encouraging. It is interesting to note that the implementation of this technology into manufacturing does not require any scientific breakthroughs. Recently, we have successfully demonstrated the feasibility of 100-mm-wide CAST ribbons. Producers of polycrystalline silicon claim that the large market projected by DOE alone will reduce the cost of this material to \$10/kg. To date, solar cells fabricated from IBM CAST ribbon have already achieved greater than eleven percent efficiency [20].

- *Technological outlook*

A reduction of the \$50/m^2 cost is possible through additional technological development. There is no doubt that such programs will lead to considerable improvement of the still "infant" ribbon technology. Several options ex-

Table 3 Correlation of electrical activity of ribbons with type of crystal defect.

Group I (strongly active)	*Group II (moderately active)*	*Group III (inactive)*
Silicon carbide dendrites and inclusions	Multiple overlapped stacking faults	First order (coherent) twins
Grain boundaries	Grown-in dislocations	Stacking faults
Degenerated twins, low-angle boundaries		
Dislocation bands		

ist, one being multi-ribbon growth. The simultaneous growth of five 75-mm-wide silicon ribbons is being pursued under a different DOE contract [21]. Multi-ribbon growth is a redoubtable task, and a breakthrough in this area would make it possible to meet the DOE objective.

A second approach is to improve the quality of the 100-mm-wide ribbon to provide greater than twelve percent solar cell efficiency. Our future work concentrates on this approach. To improve the quality of future 100-mm CAST ribbons, attempts must be made to reduce the number of electrically active defects. (The CAST ribbon electrical activities and their correlations with common crystal defects are shown in Table 3.)

Ribbons that are highly efficient at photovoltaic energy conversion can be obtained through "controlled" ribbon growth where (at least) group I defects are eliminated (see Table 3). By controlled ribbon growth we refer to control of the seeding phase, of the surface orientation, of the amount of carbon in solution, of silicon carbide formation, and of impurities in the ribbons, all factors that are obviously die-dependent. The most promising die material used so far is carbon or carbon coated with silicon carbide.

Considerable improvement in ribbon crystal quality could be achieved by control of the seeding process and resultant control of the surface orientation. So far, surface orientation of ribbons, even if obtained under steady state growth conditions, is at best fortuitous. Thus, obtaining ribbons with controlled surface orientation is clearly a major goal for all future work in ribbon growth! Otherwise, there is little hope of eliminating grain boundaries and dislocation clusters during ribbon growth.

The reduction or total elimination of SiC particles is also an important goal for future ribbon growth development. Here we have made considerable progress. In this context, clever die design leading to the high-melt-meniscus technique and the use of silicon-carbide-coated dies are helpful factors.

In conclusion, we feel that ribbon growth using the capillary action shaping technique (CAST) remains a formidable task if it must compete with the perfection level of Czochralski, float-zone, or dendritic-web crystals. Nevertheless, the CAST technique has excellent potential for reaching the DOE goal of $0.50/W. A single future breakthrough—most likely in the die material—could tip the balance in favor of CAST or other similar techniques.

Conclusions and summary

The capillary action shaping technique (CAST) for silicon ribbon growth has several potentially promising characteristics. This technique could provide continuous lengths of silicon ribbon 100 mm wide and 0.2–0.3 mm thick for continuous solar cell processing, and could eliminate the need for crystal slicing. Melt replenishment for long-ribbon growth should be achievable if the melt reservoir is thermally decoupled from the solidification front. Pulling speeds are a factor of ten or more higher than those in Czochralski growth. If ribbon crystallography is good, minority carrier lifetime values are comparable to those encountered in Czochralski crystals.

The crystal structure of CAST ribbons is inferior to that obtained with Czochralski silicon crystals. CAST crystals are plagued by uncontrolled twinning and grain boundaries, but good sections contain only parallel twinning. Such sections have excellent lifetime distributions and yield solar cells with efficiencies approaching twelve percent.

The imperfect crystal structure of some CAST ribbons relates directly to the carbon die and is attributable in part to carbon solubility in Si and in part to SiC formation.

By means of MOS *C-t* measurements, lifetime degrading defects in silicon ribbons have been classified into four groups according to the particular defect structure present and the impact of that defect on minority carrier lifetime: silicon carbide dendrites, grain boundaries, dislocations, and stacking faults. (First-order twins do not influence lifetime.)

The impact of these defects on solar cell efficiency is established, and solar cell efficiency ranges are given for the four different perfection states encountered in ribbons.

Lifetime-degrading properties of different defects are qualitatively discussed and displayed through SEM EBIC contrast by using Schottky contacts and solar cell p-n junctions.

Although the maximum ribbon growth rates are considerably higher than those for Czochralski crystals, the volume of material produced per unit time is much smaller in the case of ribbons. However, since Czochralski crystals must be sliced and subsequently polished, a large amount of the grown crystal is lost.

Economic and technological comparisons, computer-modeled at our laboratory, indicate that CAST ribbon 100 mm wide and 0.3 mm thick, obtained by a continuous growth technique, has excellent potential as a material for low cost solar cells. A cost of $\$50/m^2$ of sheet material is already feasible; further reductions are obtainable through technological improvements. The results are based on the assumption that twelve-percent-efficient solar cells can be fabricated from the 100-mm-wide ribbons.

The feasibility of 100-mm-wide CAST ribbon growth has recently been demonstrated; solar cells fabricated from CAST ribbons presently exhibit efficiencies of better than eleven percent.

Acknowledgments

This paper presents results of research performed for the Low-Cost Solar Array Project, Jet Propulsion Laboratory, California Institute of Technology, sponsored by the U.S. Department of Energy through an interagency agreement with the National Aeronautics and Space Administration.

References

1. S. N. Dermatis and J. W. Faust, Jr., *IEEE Trans. Commun. Electron.* **82,** 94 (1963).
2. D. L. Barrett, E. H. Myers, D. R. Hamilton, and A. I. Bennett, *J. Electrochem. Soc.* **118,** 952 (1971).
3. A. V. Stepanov, *Zh. Tekhnicheskoi Fiziki* **28,** 381 (1959).
4. J. Boatman and P. Goundry, *Electrochem. Technol.* **5,** 98 (1967).
5. H. E. LaBelle, Jr., *Mater. Res. Bull.* **6,** 581 (1971).
6. J. C. Swartz, T. Surek, and B. Chalmers, *J. Electron. Mater.* **4,** 255 (1975).
7. T. Surek, *J. Appl. Phys.* **47,** 4384 (1976).
8. L. C. Garone, C. V. Hari Rao, A. D. Morrison, T. Surek, and K. V. Ravi, *Appl. Phys. Lett.* **29,** 511 (1976).
9. T. F. Ciszek, *Mater. Res. Bull.* **7,** 731 (1972).
10. T. F. Ciszek and G. H. Schwuttke, *Phys. Status Solidi (A)* **27,** 231 (1975).
11. T. F. Ciszek and G. H. Schwuttke, *J. Cryst. Growth* **42,** 483 (1977).
12. G. H. Schwuttke, H. Kappert, R. Dessauer, and K. Yang, presented at the Electrochemical Society Meeting, Las Vegas, NV, October 7, 1976.
13. W. R. Bottoms, D. Gutterman, and P. Roitman, *J. Vac. Sci. Technol.* **12,** 134 (1975).
14. J. J. Lander, H. Schreiber, Jr., and T. M. Buck, *Appl. Phys. Lett.* **3,** 206 (1963).
15. W. Fahrner and C. P. Schneider, *J. Electrochem. Soc.* **120,** 100 (1976).
16. H. Lemke, *Phys. Status Solidi (A)* **12,** 125 (1965).
17. K. Yang and G. H. Schwuttke, *Technical Report 8*, Contract No. 954144, NASA Subcontract NAS7-100, Jet Propulsion Laboratory, California Institute of Technology, Pasadena, CA, July 1977.
18. A. Kran, *Proceedings of the 11th Intersociety Energy Conversion Engineering Conference*, Vol. II, American Institute of Chemical Engineers, New York, 1976, p. 1324.
19. A. Kran, *Technical Report 9*, Contract No. 954144, NASA Subcontract NAS7-100, Jet Propulsion Laboratory, California Institute of Technology, Pasadena, CA, October 1977.
20. K. W. Koliwad, private communication, Jet Propulsion Laboratory, California Institute of Technology, Pasadena.
21. F. V. Wald, *Technical Report 3*, Contract No. 954355, ERDA-Jet Propulsion Laboratory, California Institute of Technology, Pasadena, CA, July 1977.

Received November 22, 1977; revised January 12, 1978

The authors are with the IBM System Products Division at East Fishkill (Hopewell Junction), New York 12533.